



A Journal of the Gesellschaft Deutscher Chemiker

Angewandte Chemie

GDCh

International Edition

www.angewandte.org

Accepted Article

Title: Multi-mode Color-tunable Long Persistent Luminescence in Single Component Coordination Polymers

Authors: Zheng Wang, Cheng-Yi Zhu, Jun-Ting Mo, Xian-Yan Xu, Jia Ruan, Mei Pan, and Cheng-Yong Su

This manuscript has been accepted after peer review and appears as an Accepted Article online prior to editing, proofing, and formal publication of the final Version of Record (VoR). This work is currently citable by using the Digital Object Identifier (DOI) given below. The VoR will be published online in Early View as soon as possible and may be different to this Accepted Article as a result of editing. Readers should obtain the VoR from the journal website shown below when it is published to ensure accuracy of information. The authors are responsible for the content of this Accepted Article.

To be cited as: *Angew. Chem. Int. Ed.* 10.1002/anie.202012831

Link to VoR: <https://doi.org/10.1002/anie.202012831>

RESEARCH ARTICLE

Multi-mode Color-tunable Long Persistent Luminescence in Single Component Coordination Polymers

Zheng Wang^{1,2}, Cheng-Yi Zhu¹, Jun-Ting Mo¹, Xian-Yan Xu³, Jia Ruan¹, Mei Pan^{1*}, and Cheng-Yong Su¹

Abstract: Materials with tunable long persistent luminescence (LPL) properties have wide applications in security signs, anti-counterfeiting, data encrypting and other fields, which have attracted great attention. However, the majority of reported tunable LPL materials are pure organic molecules or polymers. Herein, a series of metal-organic coordination polymers displaying color-tunable LPL were synthesized by the self-assembly of HTzPTpy ligand with different cadmium halides (X = Cl, Br, and I). In solid state, their LPL emission colors can be tuned by the time-evolution, as well as excitation and temperature variation, realizing multi-mode dynamic color tuning from green to yellow or green to red, and representing the first example in single component coordination polymer materials. Single-crystal X-ray diffraction analysis and theoretical calculations reveal that the modification of LPL is due to the balanced action from single molecule and aggregate triplet excited states aroused by external heavy-atom effect. The results suggest that the rational introduction of different halide anions into coordination polymers to realize multi-color LPL is promising for different domain applications, including imaging, anti-counterfeiting and security protection.

Introduction

Long persistent luminescence (LPL) materials, also known as afterglow or long-lasting phosphorescence materials, have aroused extensive attention due to their long triplet excited state and potential applications in bioimaging,^[1] anti-counterfeiting,^[2] data encryption,^[3] light-emitting diodes,^[4] phosphorescence lasing^[5] and so forth. In the past decades, numerous materials with LPL phenomenon have been developed, including inorganic metal oxides,^[6] carbon quantum dots,^[7] perovskites,^[8] organic polymers,^[9] pure organic phosphors^[10] and metal-organic materials.^[11] Besides the pursuit of long LPL lifetime and high brightness, the controllable and tunable LPL color is another important attribute when applying these materials.^[12] However, most reported materials mainly display a single unchangeable color of LPL in the triplet state decay process. In other words, the radiative decay is universally originated from the lowest T₁ triplet excited state of the molecule. Until recently, the single component LPL color tuning was successfully achieved in a few materials such as organic small molecules,^[13] polymers^[14] and carbon dots^[15] by changing the excited

wavelengths or elapping with time, which has been applied in the logic gates and anti-counterfeiting fields.^[16-18] Nevertheless, the LPL color tuning modes in these materials are inadequate, and the hidden mechanisms are not clear. Especially, temperature-dependent color-tunable LPL materials are scarce. Therefore, it is still highly demanded to explore new types of materials with multi-mode and richful color tunable LPL performance.

Due to the low phosphorescence efficiency of most pure organic molecules, people began to apply the heavy atom effect, such as introducing heteroatoms into organic molecules or self-assembly of metal ions or clusters with organic ligands to achieve LPL emission. At present, there are a handful of reports on LPL through the synthesis of metal-organic frameworks (MOFs) or coordination polymers. Yan and coworkers used aromatic acid and metal ion of Cd²⁺/Zn²⁺ to synthesize a series of different metal-cored coordination polymers with the single green LPL in recent years.^[19] In 2019, our group reported a dynamic MOF and a series of interpenetrating MOFs, all of which show a single LPL emission color.^[11, 20] Investigating the reason behind, the monochromatic LPL is ascribed to the phosphorescence mainly produced by the triplet excited state of the single molecular ligand. On the other hand, halogen atoms are another well-known class of heavy atoms that can not only promote the intersystem crossing (ISC) to enhance the phosphorescence efficiency, but also enlarge Stokes shifts of phosphorescence. More importantly, they have potential in inducing newborn phosphorescence peak through constructing multiple intermolecular halogen-bonding (XB) interactions such as C-H...X, C-X...N, X-X and C-X...π among reported documents. Therefore, it is possible to realize polychromatic LPL emission by self-assembly of phosphor ligands with metal halides to rationally introduce halides into coordination polymers.^[21]

Based on the above considerations, a rigid ligand HTzPTpy was selected, which can potentially form the rich intra- and inter-molecular interactions in crystal state for reducing non-radiative transitions.^[22] The pure organic ligand was assembled with different CdX₂ (X = Cl, Br, I) salt under acid condition, and a series of coordination polymers with different counter anions, namely LIFM-WZ-7, LIFM-WZ-8 and LIFM-WZ-9 were synthesized and thoroughly investigated. They show different emission colors from sky blue, cyan to white light in steady state. Moreover, they are capable to exhibit rich color tuning of LPL from green to yellow or green to red after the cease of light irradiations depending on time, excitation and temperature changing modes. Combining the results of theoretical calculation and spectral analysis, the influences of heavy-atom effect of different halides on the triplet emissions, lifetimes and color adjustable LPL properties are revealed.

Results and Discussion

Synthesis and Crystal Structures

Prof. M. Pan,* Z. Wang, C.-Y. Zhu, J.-T. Mo, X.-Y. Xu, J. Ruan, C.-Y. Su
¹ MOE Laboratory of Bioinorganic and Synthetic Chemistry, Lehn Institute of Functional Materials, School of Chemistry, Sun Yat-Sen University, Guangzhou 510275, China, E-mail: panm@mail.sysu.edu.cn

² College of Chemistry and Chemical Engineering, Key Laboratory of Chemical Additives for China National Light Industry, Shaanxi University of Science and Technology, Xi'an 710021, China

³ College of Chemistry and Civil Engineering, Shaoguan University, Shaoguan 512005, China.

Supporting information for this article is given via a link at the end of the document.

RESEARCH ARTICLE

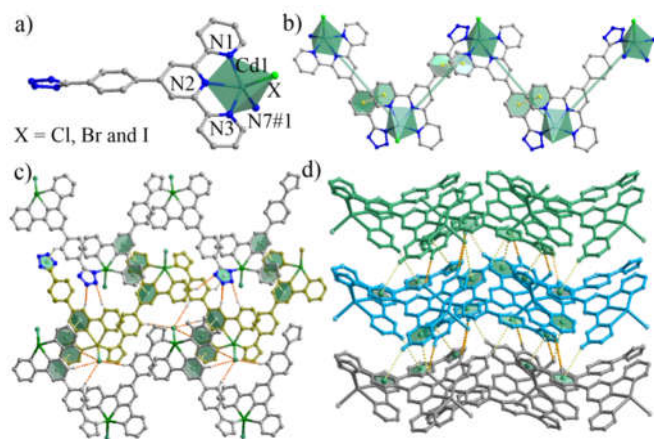


Figure 1. Crystal structure of LIFM-WZ-7-9. a) Asymmetric unit and coordination environment of Cd-center. b) Self-assembled 1D chain, c) 2D plane, and d) 3D frameworks formed via intra- and intermolecular interactions.

Reaction of CdCl_2 and HTzPTpy (molar ratio, 1:1) in DMF and water solution was carried out to afford yellow block crystals (named as LIFM-WZ-7). Using CdBr_2 and CdI_2 metal salts instead under similar conditions led to the formation of LIFM-WZ-8 and LIFM-WZ-9, respectively (Figure S1). Thermogravimetric analysis reveals that all structures can be stable up to $\sim 350^\circ\text{C}$ and the weight loss of about 3% at $\sim 170^\circ\text{C}$ corresponds to the release of one H_2O molecule from pore volume, which is in agreement with the distinct endothermic peak in the DSC curve (Figure S2 and S3). The frameworks begin to break down as the burning of the HTzPTpy units when the temperature is heated up to $\sim 350^\circ\text{C}$. The phase purity of LIFM-WZ-7-9 was confirmed by PXRD (Figure S4). Single crystal X-ray diffraction reveals that the three structures are isostructural with the similar formula $\{\text{Cd}(\text{TzPTpy})(\text{X})\cdot\text{H}_2\text{O}\}_n$ ($\text{X} = \text{Cl}, \text{Br}$ and I corresponding to LIFM-WZ-7, LIFM-WZ-8 and LIFM-WZ-9, respectively) and crystallize in the monoclinic $P2_1/n$ space group (Table S1-S3). The asymmetric unit consists of one Cd(II) center, one TzPTpy ligand, one halogen ion, and one lattice water molecule. Of which, the Cd(II) metal center is five-coordinate by three N atoms from terpyridine, which formed an equatorial plane, one N atoms from tetrazolyl and one X ion occupied the axial positions, displaying a triangular bipyramidal geometry (Figure 1a). The coordination units are further self-assembled by linker's mode of head to tail to form a 1D zig-zag chain (Figure 1b). In crystal state, intra- and intermolecular interactions play an important role in their photophysical property. As we can see, abundant intra- and intermolecular interactions including C-H...N, C-H...X and C-H... π , π - π stacking could be observed along with the (010) direction, and thus giving rise to 2D plane as shown in Figure 1c and S5. Additionally, intermolecular interactions of XB (C-H...X, C-X... π), C-H...N, C-H... π and π - π stacking between the layers linked 2D plane to a 3D supramolecular architecture (Figure 1d and S5, S6).

Photoluminescence

The ligand HTzPTpy shows a broad absorption band ranging from 200 to 450 nm, and displays blue emission in solid state at room temperature (RT) when excited with 365 nm UV light (Figure S7). The emission with maximum peak around 485 nm and short lifetime of 15.70 ns can be clearly assigned to fluorescence (Figure S8). Compared with HTzPTpy, the three coordination polymers give

different photophysical properties. The solid state UV-vis absorption spectra were measured at RT in which all three compounds show strong absorption peaks at around 350 and 460 nm, which can be attributed to single molecular transition and aggregate state transition,^[23] respectively (Figure S9). However, the three coordination polymers disclose different emission peaks in the steady-state photoluminescence spectra. When excited with 365 nm UV light, LIFM-WZ-7 exhibits dual emission bands peaked at about 448 nm and 560 nm. LIFM-WZ-8 shows two distinct emission peaks around 453 nm and 560 nm, and additionally, with a weak peak at around 610 nm. Meanwhile, LIFM-WZ-9 exhibits triple emission bands peaked at 450 nm, 560 nm and 630 nm, respectively (Figure 2a). As a result, LIFM-WZ-7-9 exhibits blue, cool white and pure white in CIE color coordinates (Figure 2b). The corresponding absolute quantum yields (Φ) of LIFM-WZ-7, LIFM-WZ-8, and LIFM-WZ-9 are 2.8%, 2.4%, and 1.4% with 365 nm excitation, respectively.

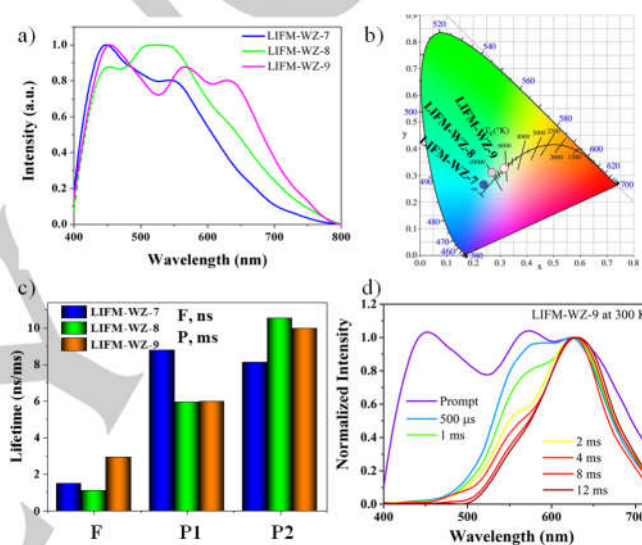


Figure 2. a, b) The emission spectra and CIE coordinates of LIFM-WZ-7-9 with the excitation of 365 nm. c) The decay lifetime of LIFM-WZ-7-9 at different emission peaks. d) TRES of LIFM-WZ-9 at 300 K.

Figure S10-S12 show the time-resolved PL decay curves of LIFM-WZ-7, LIFM-WZ-8, and LIFM-WZ-9. As we can see, the emission peaks located at high energy state around 450 nm exhibit very short lifetimes at RT, to be specific, 1.48, 1.08 and 2.83 ns for LIFM-WZ-7-9, respectively, assigning to the ligand-centered fluorescence (F, Figure 2c). However, the two emission bands of LIFM-WZ-9 peaked at ~ 560 nm and 630 nm exhibit long-lived nature with decay lifetimes of 5.96 and 9.97 ms, which can be assigned to phosphorescence and defined as P1 and P2, respectively (Figure 2c and S11). The time-resolved emission spectra (TRES) of LIFM-WZ-9 further verified the two long-lived emission bands of the frameworks (Figure 2d and S13). The results clearly show two distinct emission bands when delayed for 0.5 ms, indicating decay lifetimes of the two peaks on the order of millisecond. With the delay-time increasing, the intensity of P1 dropped rapidly. After delayed for 12 ms, the TRES of LIFM-WZ-9 mainly display P2 which possesses longer lifetime compared with P1. Similarly, the TRES of LIFM-WZ-7 and LIFM-WZ-8 exhibit long-lived P1 emission peaks around 560 nm as well, showing the lifetime of 8.79 and 5.94 ms. Meanwhile, the peaks with lower energy located at 590 and 610 nm are corresponding to P2 with the lifetime of 8.10 and 10.53 ms, respectively (Figure 2d, S11 and S13). Comparing the

RESEARCH ARTICLE

phosphorescence of LIFM-WZ-7-9, all of the P1 and P2 emissions display the same scale of millisecond lifetime, but with obviously distinct decay attributes, hinting that they might be originated from

different triplet excited states, namely, the single molecule state and aggregate state.^[24]

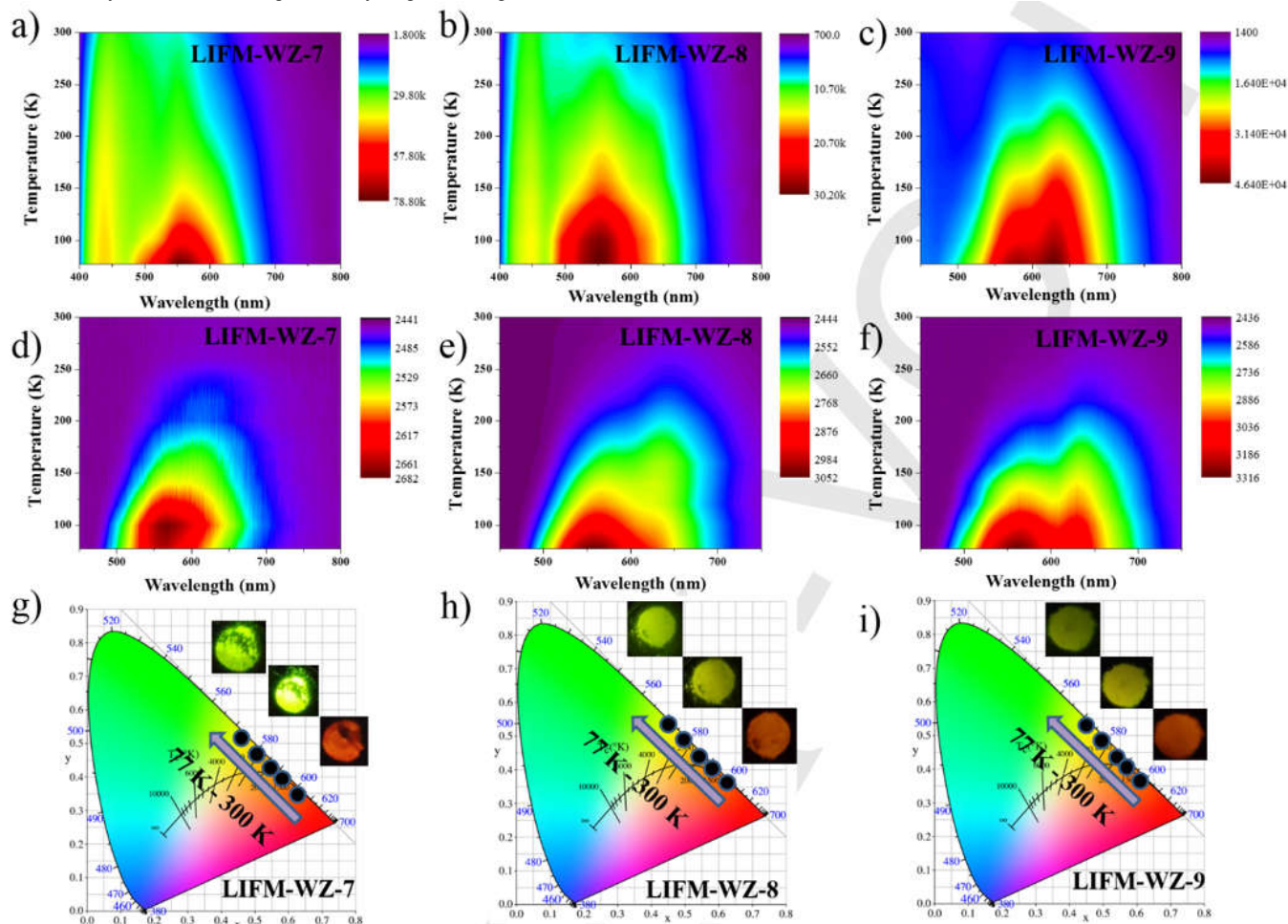


Figure 3. a-c) Temperature-dependent emission spectra of LIFM-WZ-7-9 from 300 to 77 K with the excitation wavelength of 365 nm. d-i) Temperature-dependent LPL emission spectra and CIE coordinates of LIFM-WZ-7-9 from 300 to 77 K after removal of 365 nm irradiation source of 8 ms.

In solid state, the intricate inter- and intramolecular interactions in the supramolecular coordination systems might arouse multiple emissions such as local excitation fluorescence (LE) and room temperature phosphorescence (RTP). The emission around 450 nm in LIFM-WZ-7-9 was designated as ligand-centered fluorescence from singlet energy state because of its decay lifetime of several nanoseconds. The long-wavelength emissions with lifetimes on the order of milliseconds are undoubtedly ascribed to the long-lived RTP. The two peaks around ~560 nm (P1) and ~610 nm (P2, 590, 610 and 630 nm for LIFM-WZ-7, LIFM-WZ-8 and LIFM-WZ-9, respectively) were designated as the emission of triplet phosphorescence, which can be further identified by the great enhancement at low temperature (LT, Figure 3a-c and S14, S15, Table S4). The heavy atom effect induced by cadmium and halogen containing in the coordination polymers has great influence on the energy distribution between singlet and triplet excited states. The fluorescence peaks of LIFM-WZ-7, LIFM-WZ-8 and LIFM-WZ-9 are at 448, 450, 453 nm, respectively, and all P1 emissions are located at about 560 nm. While the P2 emissions of the three coordination polymers are resided at around 590, 610, and 630 nm, respectively, which exhibit bathochromic shift trend with the increasing atomic number of halogen, indicating that halide ions might contribute to the frontier orbitals of the triplet energy

states related with P2. As we can see, the emission color of LIFM-WZ-7 to LIFM-WZ-9 can be tuned by varying the excitation wavelength from 310 to 440 nm, allowing dynamic color tuning from blue to yellow (Figure S16, Table S5, S6). Correspondingly, the excitation spectra measured at different emission wavelengths uncover a close relationship with the relative intensity of the three emission peaks (Figure S17). Typically, LIFM-WZ-7 and LIFM-WZ-9 exhibit white light emission under 360 nm and 370 nm excitation, with CIE coordinates of (0.30, 0.35) and (0.34, 0.34), respectively (Table S5), which are quite close to the CIE coordinates (0.33, 0.33) of ideal white-light emitting materials. Additionally, white light emission states were found as well when changing the temperature. LIFM-WZ-7, LIFM-WZ-8 and LIFM-WZ-9 exhibit white light emission with CIE coordinates of (0.33, 0.34), (0.32, 0.35), (0.33, 0.32) at 100 K, 140 K and 240 K, respectively (Table S7 and Figure S18).

The decay lifetimes of LIFM-WZ-7-9 under 365 nm excitation are listed in Table 1. From the lifetime data, conclusions can be drawn that the effect of halogens has different effect on the first and second phosphorescence peaks of the coordination polymers. On one hand, the halogens will significantly enhance the nonradiative transitions, leading to the decrease of emission intensity and decay lifetimes. While on the other, the introduction of heavy halogens will induce

RESEARCH ARTICLE

vibrational spin-orbit coupling (SOC), which is beneficial to raise the nonradiative rate of $T_1 \rightarrow S_0$, promote the ISC effect, and increase the efficiency of phosphorescence.

Table 1. The emission peaks and decay lifetimes of LIFM-W-7 to LIFM-WZ-9 (solid state, room temperature).

Complex	Fluorescence	P1	P2
LIFM-WZ-7	448 nm 1.48 ns	560 nm 8.79 ms	590 nm 8.10 ms
LIFM-WZ-8	450 nm 1.08 ns	560 nm 5.94 ms	610 nm 10.5 ms
LIFM-WZ-9	453 nm 2.83 ns	560 nm 5.96 ms	630 nm 9.97 ms

As a result, LIFM-WZ-7 shows the longest P1 decay lifetime of 8.79 ms in the series of LIFM-WZ-7-9. The relative short lifetimes of LIFM-WZ-8 and LIFM-WZ-9 should be caused by the nonradiative quenching effect of heavier halogens. However, for P2, LIFM-WZ-8 possesses a phosphorescence lifetime up to 10 ms, much longer than LIFM-WZ-7 and LIFM-WZ-9. This unusual phenomenon reflects the counterbalance results of nonradiative quenching and ISC increasing of halogen effect, due to the intermediate atomic weight position of Br compared with Cl and I.^[25] In brief, the introduction of heteroatoms like halogens into coordination polymers can not only construct multiple intermolecular interactions to restrict molecular motions in the solid state, but also improve the rate of ISC to boost triplet excitons phosphorescent emission, which is crucial for the generation of long persistent luminescence.

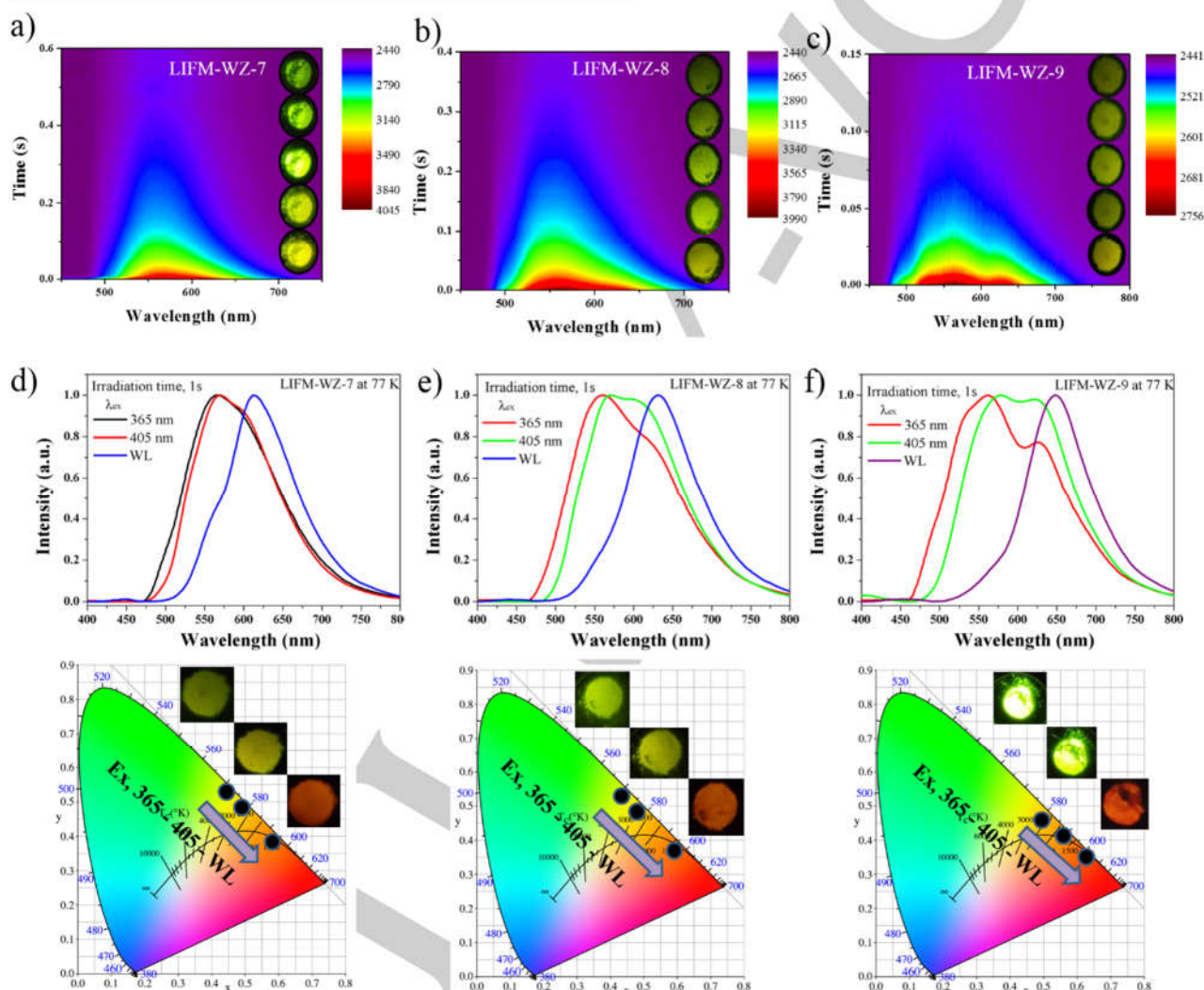


Figure 4. a-c) Time-dependent LPL emission spectra and photos of LIFM-WZ-7-9 (Inset photographs show the LPL colors change during the delay time from 8 ms to 0.6 s after removal of the UV irradiation light source). d-f) The LPL spectra (top) and CIE coordinates (down) of LIFM-WZ-7-9 after removing the 365, 405 nm and WL flash lights, respectively (Inset photographs show the LPL colors change after removal of the different irradiation light source).

Long persistent luminescence

For LIFM-WZ-9, red LPL can be obtained when removal of the 365 nm, 405 nm and white-light flashlight irradiation at RT, resulting in similar red LPL with the maximum at 650 nm (Figure S19 and S20).

However, along with a change in the temperature decreased from 300 to 77 K, the LPL exhibited an obvious hyperchromic shift from red to greenish yellow by 365 nm irradiation, in pace with a variation in the LPL maximum from 650 to 565 nm (Figure 3i, S19 and Table S8). The long-lived luminescence could still be observed several seconds after

RESEARCH ARTICLE

switch-off the excitation of a 365 nm UV lamp (Figure S21). According to the temperature-dependent LPL spectra of LIFM-WZ-9 (Figure 3f and S22), a new strong LPL peak at 565 nm emerges gradually as the temperature dropping. This results in the combination of two LPL peaks, namely, green LPL1 at 565 nm and red LPL2 at 650 nm, respectively. The same circumstances appear in LIFM-WZ-7 and LIFM-WZ-8 (Figure 3d-e, g-h and S21, S22). To figure out the origin of the dual-emission LPL spectra, temperature-dependent phosphorescence lifetimes from 300 to 77 K of LIFM-WZ-7-9 were measured (Figure S23). Through the comparative analysis of the temperature-dependent LPL spectra and temperature-dependent phosphorescence lifetime, high consistency was found in the tendency towards temperature. Specifically, all the LPL1 peaks of the three coordination polymers are located at about 565 nm, while LPL2 exhibits bathochromic-shift trend with the increasing atomic number of halogen (RT at 620, 632 and 650 nm, and LT at 615, 630, 647 nm for LIFM-WZ-7-9, respectively), which is consistent with the phosphorescence emission peaks. Therefore, the LPL1 and LPL2 peaks can be regarded as the stabilized triplet energy states of P1 and P2 (Figure S24). And due to the different emission lifetimes of

LPL1 and LPL2, the ratios of the dual-LPL bands can be observed to change in real-time during the slow decay process. In real-time detection at LT, when excited with 365 nm UV light, the LPL color of LIFM-WZ-7-9 gradually changes from yellow to green during the delay time from 8 ms to approximately 0.4 s (Figure 4a-c and Table S9).

Furthermore, similar to the steady-state emission color tuning, the two independent LPL bands give chances to tune the LPL color by adjusting the relative intensity of the two peaks through variation of the excitation wavelength. At room temperature, as removal of the 365 nm UV light, LIFM-WZ-7-9 shows green LPL, while it exhibits yellow LPL after removing the 405 nm UV light and displays red LPL when turning off the white light irradiation source. And interestingly at LT, after removing the irradiation source of white light and ultraviolet light separately, tunable LPL color from red to green was noticed at 77 K (Figure 4d-f, S21, S22 and Table S10 S11). From all the above observations, three modes of LPL color tuning are now resulted, namely, time-dependent, temperature-dependent, and excitation wavelength-dependent. To the best of our knowledge, this represents the first report of such kind of multi-mode LPL color-tuning in single component coordination polymers.

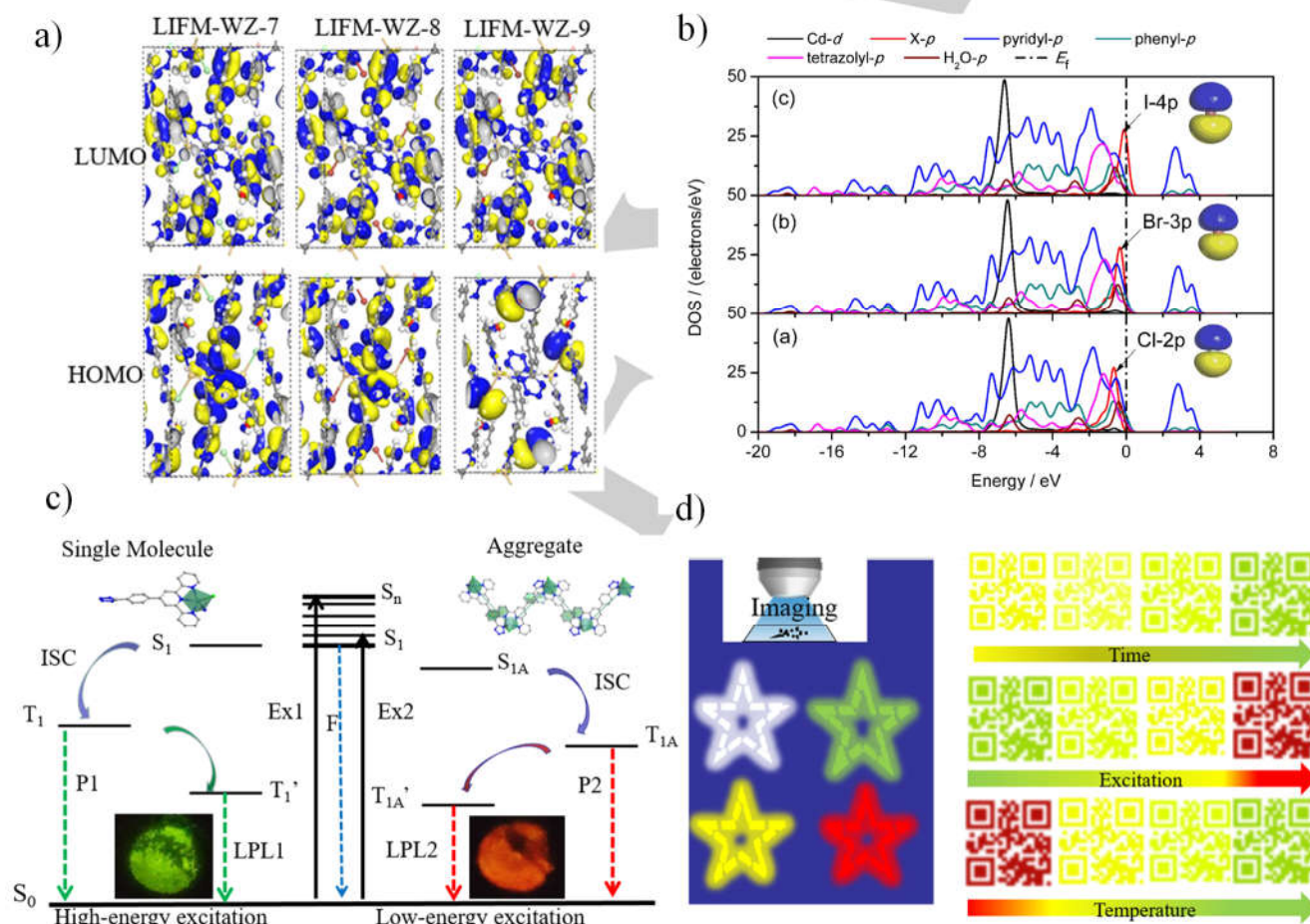


Figure 5. a) Frontier orbitals and b) TDOS/PDOS of LIFM-WZ-7-9. c) Proposed energy transfer mechanism of LIFM-WZ-7-9 (F, fluorescence; P, phosphorescence; LPL, long persistent luminescence; T₁ and T_{1'}, triplet and stabilized triplet state of single molecule; T_{1A} and T_{1A'}, triplet and stabilized triplet state of aggregate; ISC, intersystem crossing). d) Demonstration models for the application of LIFM-WZ-9 in imaging and anti-counterfeiting.

Theoretical calculation, mechanism and application

To get further insights into the mechanism of the fluorescence and dual phosphorescence/long persistent luminescence in LIFM-WZ-7-9,

theoretical calculations were carried out by periodic density functional theory (PFT) using Material Studio software. For LIFM-WZ-7 and LIFM-WZ-8, the frontier orbital analysis reveals that the highest occupied molecular orbitals and the lowest unoccupied molecular

RESEARCH ARTICLE

orbitals are mainly located at the phenyl-tetrazole and terpyridine groups of the TzPTpy ligand, respectively (Figure 5a). This suggests that the photoemission including fluorescence (F) and P1 are mainly derived from the TzPTpy units within the framework. However, for LIFM-WZ-9, the lowest unoccupied molecular orbitals are mainly located at the terpyridine groups of the TzPTpy ligand, while the highest occupied molecular orbitals distributed in iodine atom, which is different from LIFM-WZ-7-8. Comparatively, iodine as the heaviest atom weight has the strongest SOC ability to populate the triplet state, while bromine and chlorine belong to the halogen which should have a similar effect, although they have relative weaker and moderate SOC ability. This is further reflected on the different P2 and LPL2 properties associated with the halogen-involved aggregate emissions in LIFM-WZ-7-9. Total/partial electronic density of states (TDOS and PDOS) showed that the band gaps for LIFM-WZ-7-9 are 2.53, 2.50 and 2.40 eV, respectively. This is in accordance with the bathochromic shift color of LIFM-WZ-7-9. Moreover, we can see from the projected density of states that in the vicinity of the Fermi level, from Cl to Br and I in LIFM-WZ-7-9, the p orbital of the halogen valence electron layer displays a trend of red shift, which is consistent with the electronegativity of halogen atoms. That is, halogens with high electronegativity are not easy to lose electrons, while halogens with low electronegativity exhibits high metallicity and need low energy to lose electrons (Figure 5b). This is also in consistent with the experimental results that the P2 and LPL2 in LIFM-WZ-7-9 shows a steady red-shift with the change of halogen counter ions from Cl, Br to I.

From the combination of both experimental and computation, it is informative to designate the multiple emissions and energy-transfer mechanisms in LIFM-WZ-7-9 (Figure 5c): First, the ligand molecules in the coordination polymers absorb different wavelength energy of 365, 405 nm and WL and transfer it to the excited singlet states S_1 , which can emit blue fluorescence (F). And then, through effective ISC from S_1 to the excited triplet states T_1 of the single molecule, green phosphorescence (P1) is generated, while red phosphorescence (P2) is generated from the triplet energy (T_{1A}) of the aggregate state in the frameworks. Afterwards, the T_1 and T_{1A} states relax further to the lower-energy T_1' and T_{1A}' states after turning off the light irradiation, leading to the green LPL1 and red LPL2, respectively.

The observation of the excitation and temperature-dependent LPL color change in LIFM-WZ-7-9 further manifests the above dual-phosphorescence assignments, and also reflects the heavy-atom effect by the introduction of halogens. As we can see, all LPL1 peaks of LIFM-WZ-7-9 locate at around 565 nm which are slightly affected by the counter anions, suggesting that the halogens participate little in the frontier orbitals of the triplet energy (T_1) of the ligand single molecule state. Meanwhile, the lifetime of P1 peaks under cryogenic condition of LIFM-WZ-7, LIFM-WZ-8 and LIFM-WZ-9 are 323.7, 216 and 35.3 ms with 365 nm excitation, respectively, which are longer than that of P2. Therefore, the single molecule triplet state phosphorescence P1 and LPL1 is dominant at 77 K, due to the fact that the LT restricted the molecular motion and suppressed the non-radiative transition which is sharply consumed at RT. However, the P2 of LIFM-WZ-7-9 are located at 590, 610 and 630 nm, and the LPL2 are located at 620, 632 and 650 nm, respectively, displaying the bathochromic-shift trend of the triplet energy (T_{1A}) of the aggregate state due to the introduction of halogens with increasing atomic number. Moreover, compared with the lifetimes of P1 at RT and 77 K, the P2 lifetimes increase more moderately as the temperature decreases, as a result of the competing effects of nonradiative quenching and ISC increasing by the introduction of the halogens.

Furthermore, the irradiation energy is also decisive to the phosphorescence and LPL attributes in the halogen-introduced coordination polymers. Generally speaking, high energy UV irradiation and low temperature condition is beneficial to the dominance of P1 and LPL1 from the single molecule excited state, while low energy white light irradiation and high temperature leads to the dominance of P2 and LPL2 from the aggregate state.

The above multiple photophysical and especially color-tuning LPL emissions of LIFM-WZ-7-9 can be applied for different purposes. Here, we choose LIFM-WZ-9 as the representative illustration. On the basis of the white color emission under excitation of 365 nm, the green, yellow and red LPL emission after removal of 365, 405 and white light irradiation source, different color images of the pentagram were created by varying the external irradiation. In addition, multi-color 2D code were designed with the multi-mode LPL color tuning by time-evolution, variable-temperature and change of excitation wavelengths (Figure 5d), showing great potentials for the application in camouflaging and imaging, respectively.

Conclusion

In summary, we have designed and synthesized a series of coordination polymers incorporated with different halogen anions. All of them display multi-emission peaks and photoluminescent colors changing from blue, white to yellow. Importantly, all of them show multi-color LPL due to the interplay of triplet emissions from single molecule and aggregate state. The high energy green LPL comes from the single molecule phosphorescence (P1) restricted by intermolecular and intramolecular interactions, while the low energy red LPL is contributed by the aggregate state phosphorescence (P2) induced by supramolecular accumulation and halogen bonding. Especially, the action of halogen ions in the coordination polymers brings counter-balanced effects of nonradiative quenching and ISC increasing, which can change the relative intensities and lifetimes of the two phosphorescence. As a result, by time evolution as well as temperature and excitation variation, the total LPL colors of the coordination polymers are tunable from green to red. This research not only provides a basic design strategy for implementing multi-mode color-tunable LPL in single-component coordination polymers, but also provides an opportunity to develop a new platform for multicolor display, forgery, and other potential applications.

Acknowledgements

This work was supported by NSFC (21771197, 21821003, 21720102007, 21890380), Local Innovative and Research Teams Project of Guangdong Pearl River Talents Program (2017BT01C161), and FRF for the Central Universities.

Keywords: Color tuning • Long persistent luminescence • Coordination polymers

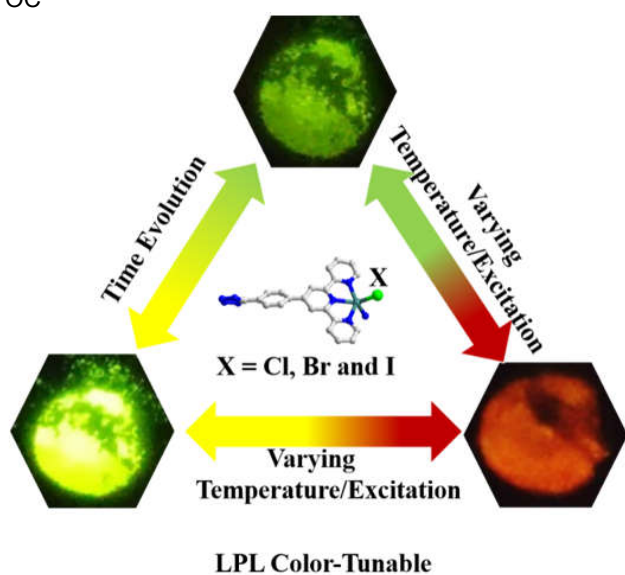
- [1] a) T. Maldiney, A. Bessiere, J. Seguin, E. Teston, S. K. Sharma, B. Viana, A. J. Bos, P. Dorenbos, M. Bessodes, D. Gourier, D. Scherman, C. Richard, *Nat. Mater.* **2014**, *13*, 418-426; b) X. Zhen, C. Xie, K. Pu, *Angew. Chem. Int. Ed.* **2018**, *57*, 3938-3942; c) C. Xie, X. Zhen, Q. Miao, Y. Lyu, K. Pu, *Adv. Mater.* **2018**, *30*, 1801331.
- [2] Z. Wang, C. Y. Zhu, S. Y. Yin, Z. W. Wei, J. H. Zhang, Y. N. Fan, J. J. Jiang, M. Pan, C. Y. Su, *Angew. Chem. Int. Ed.* **2019**, *58*, 3481-3485.

RESEARCH ARTICLE

- [3] a) K. Jiang, L. Zhang, J. Lu, C. Xu, C. Cai, H. Lin, *Angew. Chem. Int. Ed.* **2016**, *55*, 7231-7235; b) X. Wang, H. L. Ma, M. X. Gu, C. Q. Lin, N. Gan, Z. L. Xie, H. Wang, L. F. Bian, L. S. Fu, S. Z. Cai, Z. G. Chi, W. Yao, Z. F. An, H. F. Shi, W. Huang, *Chem. Mater.* **2019**, *31*, 5584-5591.
- [4] S. Hirata, K. Totani, J. X. Zhang, T. Yamashita, H. Kajji, S. R. Marder, T. Watanabe, C. Adachi, *Adv. Funct. Mater.* **2013**, *23*, 3386-3397.
- [5] Z. Yu, Y. Wu, L. Xiao, J. Chen, Q. Liao, J. Yao, H. Fu, *J. Am. Chem. Soc.* **2017**, *139*, 6376-6381.
- [6] P. Wang, X. Xu, D. Zhou, X. Yu, J. Qiu, *Inorg. Chem.* **2015**, *54*, 1690-1697.
- [7] L. Q. Bai, N. Xue, X. R. Wang, W. Y. Shi, C. Lu, *Nanoscale* **2017**, *9*, 6658-6664.
- [8] a) Z. Gong, W. Zheng, Y. Gao, P. Huang, D. Tu, R. Li, J. Wei, W. Zhang, Y. Zhang, X. Chen, *Angew. Chem. Int. Ed.* **2019**, *58*, 6943-6947; b) S. Yang, D. Wu, W. Gong, Q. Huang, H. Zhen, Q. Ling, Z. Lin, *Chem. Sci.* **2018**, *9*, 8975-8981.
- [9] a) C. Zhao, Y. Jin, J. Wang, X. Cao, X. Ma, H. Tian, *Chem. Commun.* **2019**, *55*, 5355-5358; b) N. Jiang, G. F. Li, B. H. Zhang, D. X. Zhu, Z. M. Su, M. R. Bryce, *Macromolecules* **2018**, *51*, 4178-4184.
- [10] A. Forni, E. Lucenti, C. Botta, E. Cariati, *J. Mater. Chem. C* **2018**, *6*, 4603-4626.
- [11] Z. Wang, C.-Y. Zhu, Z.-W. Wei, Y.-N. Fan, M. Pan, *Chem. Mater.* **2019**, *32*, 841-848.
- [12] a) S. Pan, Z. Chen, X. Zheng, D. Wu, G. Chen, J. Xu, H. Feng, Z. Qian, *J. Phys. Chem. Lett.* **2018**, *9*, 3939-3945; b) J. Wang, Z. Chai, J. Wang, C. Wang, M. Han, Q. Liao, A. Huang, P. Lin, C. Li, Q. Li, Z. Li, *Angew. Chem. Int. Ed.* **2019**, *58*, 17297-17302; c) T. Ai, W. Shang, H. Yan, C. Zeng, K. Wang, Y. Gao, T. Guan, C. Fang, J. Tian, *Biomaterials* **2018**, *167*, 216-225.
- [13] L. Gu, H. F. Shi, L. F. Bian, M. X. Gu, K. Ling, X. Wang, H. L. Ma, S. Z. Cai, W. H. Ning, L. S. Fu, H. Wang, S. Wang, Y. R. Gao, W. Yao, F. W. Huo, Y. T. Tao, Z. F. An, X. G. Liu, W. Huang, *Nat. Photonics* **2019**, *13*, 406-411.
- [14] Z. Wang, Y. Zhang, C. Wang, X. Zheng, Y. Zheng, L. Gao, C. Yang, Y. Li, L. Qu, Y. Zhao, *Adv. Mater.* **2020**, *32*, 1907355.
- [15] C. Wang, Y. Chen, T. Hu, Y. Chang, G. Ran, M. Wang, Q. Song, *Nanoscale* **2019**, *11*, 11967-11974.
- [16] S. Zheng, T. Zhu, Y. Wang, T. Yang, W. Z. Yuan, *Angew. Chem. Int. Ed.* **2020**, *59*, 10018-10022.
- [17] J. X. Wang, Y. G. Fang, C. X. Li, L. Y. Niu, W. H. Fang, G. Cui, Q. Z. Yang, *Angew. Chem. Int. Ed.* **2020**, *59*, 10032-10036.
- [18] H. Wang, H. Shi, W. Ye, X. Yao, Q. Wang, C. Dong, W. Jia, H. Ma, S. Cai, K. Huang, L. Fu, Y. Zhang, J. Zhi, L. Gu, Y. Zhao, Z. An, W. Huang, *Angew. Chem. Int. Ed.* **2019**, *58*, 18776-18782.
- [19] a) D. Li, X. Yang, D. Yan, *ACS Appl. Mater. Interfaces* **2018**, *10*, 34377-34384; b) Y. Yang, K. Z. Wang, D. Yan, *ACS Appl. Mater. Interfaces* **2017**, *9*, 17399-17407; c) X. Yang, D. Yan, *Adv. Opt. Mater.* **2016**, *4*, 897-905; d) Y. Yang, K. Z. Wang, D. Yan, *ACS Appl. Mater. Interfaces* **2016**, *8*, 15489-15496.
- [20] Z. Wang, C. Y. Zhu, P. Y. Fu, J. T. Mo, J. Ruan, M. Pan, C. Y. Su, *Chem. Eur. J.* **2020**, *26*, 7458-7462.
- [21] a) W. Wang, Y. Zhang, W. J. Jin, *Coordin. Chem. Rev.* **2020**, *404*, 213107; b) E. Lucenti, A. Forni, C. Botta, C. Giannini, D. Malpicci, D. Marinotto, A. Previtali, S. Righetto, E. Cariati, *Chem. Eur. J.* **2019**, *25*, 2452-2456.
- [22] R. Li, S.-H. Wang, Z.-F. Liu, X.-X. Chen, Y. Xiao, F.-K. Zheng, G.-C. Guo, *Cryst. Growth & Des.* **2016**, *16*, 3969-3975.
- [23] K. Kanosue, S. Ando, *Acs Macro. Letters* **2016**, *5*, 1301-1305.
- [24] a) Z. He, W. Zhao, J. W. Y. Lam, Q. Peng, H. Ma, G. Liang, Z. Shuai, B. Z. Tang, *Nat. Commun.* **2017**, *8*, 416; b) C. J. Zhou, S. T. Zhang, Y. Gao, H. C. Liu, T. Shan, X. M. Liang, B. Yang, Y. G. Ma, *Adv. Funct. Mater.* **2018**, *28*, 1802407.
- [25] H. Ma, Q. Peng, Z. An, W. Huang, Z. Shuai, *J. Am. Chem. Soc.* **2019**, *141*, 1010-1015.

RESEARCH ARTICLE

TOC



By delicate design of coordination polymers incorporating different halogens, multi-mode color-tunable long persistent luminescence (LPL) from green to yellow or green to red were successfully achieved. Specifically, the LPL emission colors can be tuned by time, excitation and temperature, revealing the counter-balanced mechanisms from single molecule and aggregate triplet excited states aroused by external heavy-atom effect.

Accepted Manuscript